

DO ROTATION CURVES OF SPIRAL GALAXIES IN CLUSTERS DECLINE?¹

P. AMRAM,² W. T. SULLIVAN III,³ C. BALKOWSKI,⁴ M. MARCELIN,² AND V. CAYATTE⁴

Received 1992 June 15; accepted 1992 November 12

ABSTRACT

Rotation curves for 21 spiral galaxies in five clusters have been obtained in a search for possible effects of the cluster environment on individual galaxy dynamics. We find no significant evidence for anything more than a small influence of the cluster environment. In particular, using 12 selected galaxies we do not confirm the strong correlation between slope of rotation curve and location within a cluster reported by Whitmore, Fobes, & Rubin.

Subject headings: galaxies: clustering — galaxies: kinematics and dynamics

1. PRELUDE

Over the past decade many effects of the cluster environment on member galaxies have been established. These effects are manifest in the amount and distribution of gas in cluster spirals, the luminosity and light distributions within galaxies, and the segregation of morphological types. The present study focuses on the dynamics of spiral galaxies in clusters by examining whether or not their rotation curves differ systematically from those in the field. Our observations were undertaken in response to the papers by Rubin, Whitmore, & Ford (1988) and Whitmore, Forbes, & Rubin (1988; hereafter collectively referred to as RWF). RWF presented evidence for a correlation in the sense that inner cluster spirals tended to have falling rotation curves, unlike those of outer cluster spirals or the great majority of field spirals. If correct, this result would be of great importance, for it would provide clues to the origin and nature of the massive halos of dark matter that are invoked to account for the lack of decline in most measured rotation curves. In particular, RWF pointed out that their declining rotation curves suggested that dark matter halos were absent from cluster spirals, either because the halos had become stripped by interactions with other galaxies or with an intracluster medium, or because the halos had never formed in the first place.

We have measured the rotation curves for a large sample of spiral galaxies in five clusters. These rotation curves have been constructed from detailed two-dimensional maps of each galaxy's velocity field as traced by emission from the H α line. This complete mapping, combined with the sensitivity of our observations, allows the construction of high-quality rotation curves. In the following section we briefly discuss the acquisition and reduction of these data. Section 3 then presents our analysis of a first sample of 21 rotation curves, followed by discussion in § 4. These results have been presented in a preliminary form by Amram et al. (1991a, b) and in the thesis of Amram (1991).

2. THE DATA

Clusters and galaxies were chosen on the basis of the following criteria: a good mix of types of clusters and of spiral gal-

axies, sufficient angular sizes and anticipated signal levels (Kennicutt, Bothun, & Schommer 1984), a range of galaxy locations within each cluster, existence of previous H I and photometric data (Bothun et al. 1985; Sullivan 1989), and overlap with the sample of RWF. We have observed six galaxies in common with RWF in Cancer, Pegasus I, and Hercules (A2151). In addition we have observed spirals in Coma (A1656) and A539. These clusters span a range of properties from those of Coma (very populous and centrally concentrated, dominated by elliptical galaxies, high velocity dispersion, hot intracluster medium) to those of Peg I (loose aggregation of mostly spiral galaxies, low dispersion, no intracluster medium). Table 1 provides the basic measurements for our first sample of 21 galaxies in five clusters. In the present paper we assume $H_0 = 75 \text{ km s}^{-1} \text{ Mpc}^{-1}$.

Column (1) of Table 1 gives the cluster name and distance (from RWF for clusters in common, and from Bothun et al. 1985 for A539 and Coma), and column (2) is the galaxy name. Columns (3), (4), and (5) give the morphological type, inclination, and total blue luminosity ($M_\odot = 5.48$) from the *Third Reference Catalogue of Galaxies* (de Vaucouleurs et al. 1991, hereafter RC3), except where noted. Column (6) is the radius of the galaxy at the 25 mag arcsec⁻² B isophote, corrected for galaxian and galactic extinction according to the precepts of the RC3 (except where noted), and column (7) is the distance on the major axis to the farthest measured point on our rotation curve. Columns (8) and (9) contain the outer gradient and total gradient of the rotation curve (defined below), and column (10) is the projected distance to the cluster center; centers are from Struble & Rood (1987) for A539 and Coma, from Bothun et al. (1983) for Cancer, and from Bothun et al. (1985) for Peg I and A2151. Column (11) gives the projected density of neighboring galaxies in the style of Dressler (1980); the specific definition is discussed below. Finally, column (12) indicates the sample to which each galaxy belongs. Sample 1 contains the most reliable rotation curves for studying any environmental effect. Sample 2 contains galaxies with inclinations greater than 65° and therefore having possible problems with internal extinction. Measured rotation curves in this case usually exhibit artificially high slopes because one detects the gas preferentially on the near side of the galaxy. Sample 3 galaxies are questionable due to the presence of companion galaxies (and therefore possible tidal effects), evidence for non-circular motions, or rotation data requiring extrapolation (and therefore less certain). We have defined these samples in this manner in order to attempt to isolate any environmental effect

¹ Based on observations obtained at the Canada-France-Hawaii Telescope.

² Observatoire de Marseille, 2 place Le Verrier, F-13248 Marseille Cedex, France.

³ Department of Astronomy, University of Washington, Seattle, WA 98195.

⁴ Observatoire de Meudon, DAEC, F-92195, Meudon, France.

TABLE 1
ROTATION CURVES OF CLUSTER SPIRALS

| Cluster (1) | Galaxy ^a (2) | <i>T</i> (3) | <i>i</i> (4) | log <i>L</i> (<i>L_B</i> ⊙) (5) | <i>R</i> ₂₅ (6) | <i>R</i> _{me} (7) | OG (8) | TG (9) | <i>R</i> _{cl} (Mpc) (10) | Density (Mpc ⁻²) (11) | Sample (12) |
|--------------------------------|----------------------------|-----------------|-----------------|--|-------------------------------|-------------------------------|-----------|-----------|---|---|----------------|
| A539 (<i>D</i> = 114 Mpc) | U3269 | 4 | 50° | 10.7 | 27" | 25" | 7% | ... | 1.2 | 1.6 | 1 |
| | U3282 | 6 | 50 | 10.7 | 34 | 37 | 5 | 6% | 0.86 | 2.6 | 1 |
| Cancer (<i>D</i> = 61 Mpc) | Z119-043 | ... | 65 | 9.8 ^b | 18 ^b | 21 | 20 | 43 | 0.47 | 0.65 | 2 |
| | U4329 ^c | 6 | 50 | 10.2 | 63 | 89 | -4 | 0 | 0.44 | 0.64 | 1 |
| | N2558 ^c | 2 | 55 | 10.4 | 55 | 56 | 2 | 4 | 0.69 | 0.73 | 1 |
| | Z119-053 | ... | 50 | 9.7 ^b | 21 ^b | 23 | 6 | 11 | 0.32 | 0.70 | 1 |
| | U4386 ^c | 3 | 80 | 10.4 | 57 | 56 | 24 | ... | 0.91 | 0.86 | 2 |
| Coma (<i>D</i> = 93 Mpc) | N2595 | 5 | 31 | 10.7 | 97 | 80 | 6 | ... | 1.9 | 0.56 | 1 |
| | N4848 | 2 | 65 | 10.7 | 49 | 26 | ... | ... | 0.76 | 7.3 | 3 |
| | Z160-058 | 5 | 75 | 10.3 | 31 | 35 | 19 | 35 | 2.9 | 10.1 | 2 |
| | N4911 | 4 | 30 | 10.8 | 43 | 29 | ... | ... | 0.61 | 16 | 3 |
| | N4921 | 2 | 40 | 11.0 | 74 | 53 | 22 | ... | 0.76 | 25 | 3 |
| A2151 (<i>D</i> = 149 Mpc) | Z160-106 ^d | -2 | 45 | 10.2 ^b | 18 ^b | 17 ^e | 35 | 43 | 1.15 | 7.7 | 3 |
| | Z130-008 | 6 | 52 | 10.0 | 13 | 20 | 21 | 32 | 4.9 | 0.22 | 1 |
| | U10085 | 6 | 50 | 10.8 | 31 | 41 | 8 | 0 | 7.3 | ... | 1 |
| Peg I (<i>D</i> = 54 Mpc) | N6045 ^c | 5 | 75 | 11.0 | 40 | 39 | 10 | ... | 0.14 | ... | 3 |
| | N7536 | 4 | 72 | 10.3 | 60 | 74 | 13 | 12 | 5.2 | 0.14 | 2 |
| | N7593 | 5 | 51 | 10.1 | 31 | 37 | 7 | 16 | 3.0 | 0.21 | 1 |
| | U12498 ^{e,d} | 3 | 63 | 10.1 | 42 | 41 | -7 | ... | 0.26 | 7.3 | 1 |
| | N7631 ^c | 3 | 64 | 10.4 | 56 | 75 | 4 | 16 | 0.29 | 5.0 | 1 |
| | N7643 | 5 | 59 | 10.2 | 43 | 34 | 5 | ... | 3.6 | 0.19 | 1 |

^a U = UGC, N = NGC, Z = Zwicky.

^b Data not from RC3.

^c Also observed by RWF.

^d Z160-106 = N4926A; U12498 = IC 5309.

^e Distance measured on side away from companion.

from other known effects on rotation curves. Note that the galaxies in each of the three samples occur in both the inner and outer parts of the clusters.

Our rotation curves were deduced from observations obtained with the 3.6 m Canada-France-Hawaii Telescope on Mauna Kea in 1989–1990. The H α velocity fields were obtained with the “Palila” scanning Fabry-Perot interferometer inside a focal reducer at the Cassegrain focus, followed by a CCD that provided a 5' field of view and a $\sim 1''.5$ pixel size. The free spectral range was 257 km s⁻¹, and the tuning of the interference plates was such that velocity channel maps spaced by 11 km s⁻¹ could be constructed. Observing time for each of the galaxies (which ranged from thirteenth to fifteenth magnitude) was typically 2 hr. Data reduction involved calibration via a neon lamp, subtraction of the night-sky background (which is usually the limiting factor in determining profile baselines and therefore velocities), subtraction of continuum emission from the galaxy, and careful inspection of the individual line profiles detected in each of several hundred pixels. For those channels in each pixel deemed to have a sufficient signal-to-noise ratio, a velocity was defined as the intensity-weighted mean of the emission profile. The accuracy of the velocity determination for an individual pixel is typically 10–20 km s⁻¹.

In order to derive a rotation curve from the velocity field, repeated trials were conducted with differing values of dynamic center, systemic velocity, position angle of major axis, and inclination of the disk. The final values for these parameters, which determine the rotation curve, are based on symmetrizing, minimizing, and optimizing the residuals expected from a model of circular rotation in an inclined disk (e.g., see Warner, Wright, & Baldwin 1973). All pixels within 80° of the major

axis, suitably deprojected and then weighted in the final solution according to geometric factors (lower weights for off-axis pixels), went into this determination. Figure 1 illustrates the rotation curve of a typical galaxy. Full details and plots of all our measurements are given by Amram (1991) and Amram et al. (1992).

3. PRELIMINARY ANALYSIS

Following RWF, we characterize the slope of a rotation curve with reference to fiducial points defined relative to the optical radius *R*₂₅. The “outer gradient” (OG) is the change in

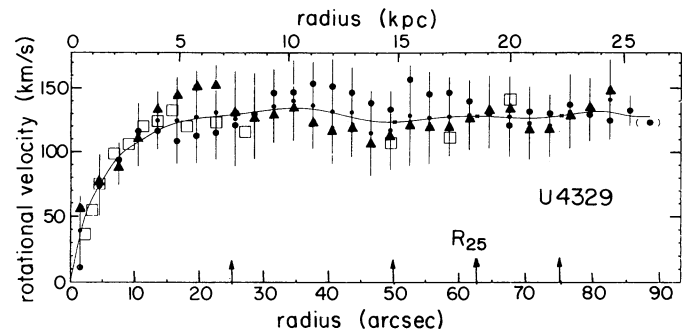


FIG. 1.—Rotation curve for U4329 in the Cancer cluster. The isophotal radius *R*₂₅ is indicated, as well as 0.4, 0.8, and 1.2 *R*₂₅. Large solid circles represent the weighted mean values of rotation velocities in successive annuli in the plane of the galaxy on the receding side; triangles represent the approaching side, and the small filled circles are the overall means, through which a spline function has been fitted. The error bars on each mean value represent $\pm 1 \sigma$ in the distribution of measured pixels making up that mean. The error in the mean is typically lower by a factor of 3–7. Large open boxes are the data points along the major axis measured by RWF.

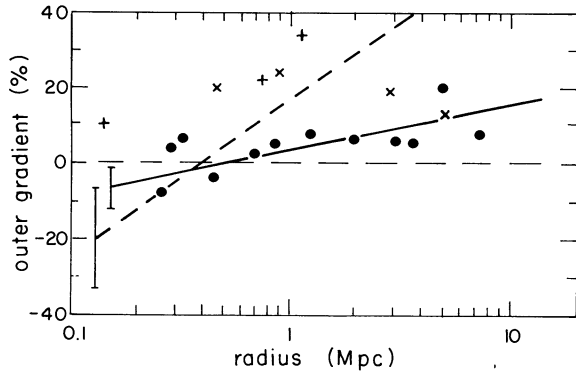


FIG. 2.—Outer gradient (OG) for each galaxy vs. its projected radius from its cluster center. Three samples are distinguished (see text for definitions): sample 1 (the most reliable data) with filled circles and a least-squares linear fit (solid line), sample 2 (crosses), and sample 3 (plus signs). The error in each OG value is typically $\pm 10\%$. The dashed line shows the fit published by RWF, when converted to our distance scale. Error bars for ± 1 rms are shown for both the RWF fit and ours.

rotation velocity between 0.4 and 0.8 times R_{25} , normalized to the maximum measured velocity and expressed as a percentage. For our sample we employ OG as well as a “total gradient” (TG), similarly defined between 0.4 and $1.2R_{25}$. RWF present evidence for falling rotation curves in the central regions of clusters, as well as for a marked correlation between OG and r_{cl} , the projected distance of each galaxy from its cluster center. In Figure 2 we present the same plot for our sample. The obtained correlation is $OG = (12.6 \pm 5.4) \log R + 4.3$ with a correlation coefficient of 0.67 and a probability of 98.4% that this correlation exists. The slope is the mean value of the least-squares fits of y upon $\log x$ and $\log x$ upon y ; the uncertainty is the 1σ value. Our slope is only 31% of that found by RWF (see Fig. 2), so that any effect that may be present in our sample is relatively small. Our data, especially if combined with those of RWF, are also consistent with the hypothesis that an effect exists only for those galaxies within 0.5 Mpc of the cluster center, but a larger sample of good quality inner galaxies is needed to establish this.

A plot similar to Figure 2 for TG also shows a weak effect at most. Our results hold whether or not we confine ourselves to our 12 best galaxies (sample 1 in Table 1, shown as filled dots in Fig. 2) or we include the seven other galaxies that are questionable. Note also that we have only two falling rotation curves (OG values of -4% and -7%) in our total OG sample of 19 galaxies, in contrast to the RWF data set where six of 16 spirals have negative values of OG, ranging as low as -26% . The galaxies in common between the two samples provide an illustrative test: for example, we find OG to be -4% for U4329 (Fig. 1), and RWF obtain -12% (based on the large open boxes in Fig. 1).

The reasons for this discrepancy with RWF probably arise in the following manner. First, our rotation curves are based on the entire velocity field, as opposed to RWF’s data from a $1''$ wide slit along the major axis, for which gaps in line-emitting gas along the major axis cause problems (see Fig. 1). Furthermore, galaxy position angle and inclination can be derived for our data from the galaxy kinematics themselves, but with slit data these can only be based on the shape of the optical image. A second reason for differences with RWF is that the Fabry-Perot/CCD technique is more sensitive than a traditional spectrograph with image tube and photographic plate. Indeed, this has allowed us to measure rotation velocities typically

15%–30% farther from the nucleus than RWF, and thus better to estimate the general run of each rotation curve and its gradient. Third, we have eliminated from our sample 1 all edge-on, interacting, and distorted galaxies; on the other hand, RWF include in their sample many such galaxies, which we argue are ill suited for the present purposes.

The clusters in both our sample and that of RWF have a wide range of sizes and populations, and combining all clusters in a single plot of OG versus r is fraught with difficulties. Another parameter for testing possible influences of the various clusters’ environments is the projected density of neighboring galaxies (hereafter simply called “density”) as first studied by Dressler (1980). We have defined this density in terms of the five nearest galaxies from the *Catalog of Galaxies and of Clusters of Galaxies* (Zwicky et al. 1961–68) with luminosities larger than that corresponding to the Zwicky catalog limiting magnitude of 15.7 at the distance of A539 (values for the more distant A2151 have therefore not been calculated because of incompleteness). This quantity is tabulated in Table 1, and in Figure 3 is plotted versus the outer gradient OG. Consistent with our previous results, a linear fit yields a weak trend of flatter rotation curves in denser regions, although the data of sample 1 are also consistent with the presence of no effect at all. A larger sample is needed to confirm if the apparent trend is significant. A similar result is obtained if the density is defined in terms of the 10 nearest Zwicky galaxies.

4. CONCLUSION

We have found no biases in our sample in luminosity, morphological type, inclination, or size that might affect our main result of no significant environmental effect. For instance, Persic & Salucci (1991) have shown that slopes of rotation curves strongly correlate with luminosities, but normalizing our measured slopes for the luminosity of each galaxy does not change the result. We also find that our conclusions hold for other definitions of rotation curve slope, such as TG and the “delta” parameter of Persic & Salucci (1991). We have likewise found no significant effects on our sample arising from any of the correlations discussed by Casertano & van Gorkom (1991) between galaxian properties and the slope of 21 cm H I rotation curves.

Our results are also consistent with the single-slit rotation

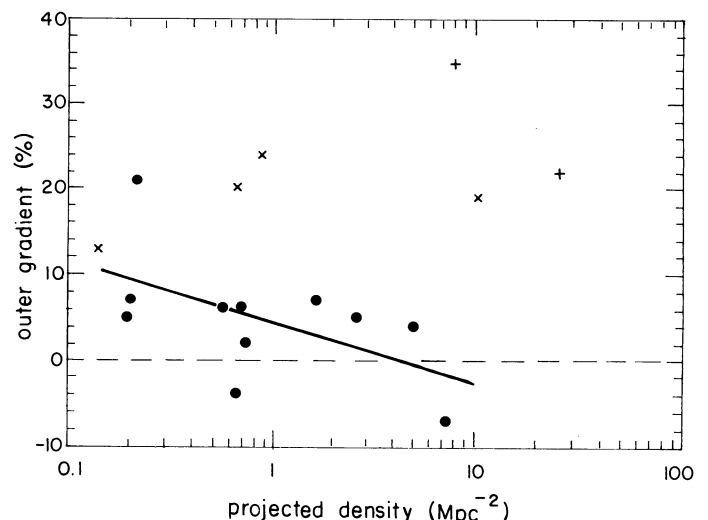


FIG. 3.—OG vs. projected density of the nearest five galaxies; see text for details. Symbols are as in Fig. 2.

curves reported for the Virgo cluster by Distefano et al. (1990), which show no dependence of OG on distance from that cluster center. RWF also did photometry for their galaxies and derived the run of M/L with radius in each galaxy, finding that M/L rose much more weakly for galaxies in the inner regions of clusters. They presented this as further strong evidence in favor of a lack of dark halos around inner galaxies. Unfortunately, we have no photometry for our own galaxies with which to check this result, but we are now obtaining such data. We have also recently observed about 15 more rotation curves in the present clusters and in A262 and A1367.

We thank the entire CFHT staff, in particular Robin Arsenault, Guy Monnet, and B. Grundseth, for their strong support of this project. Etienne Le Coarer's and J. Boulesteix's software systems were indispensable for the data reduction. We thank Mark Hammergren for assistance with the data analysis. W. T. S. and C. B. acknowledge a NATO Collaborative Research Grant, and W. T. S. thanks the American Astronomical Society for partial support through its Small Research Grant program. This work has also been supported by the Groupement de Recherche "Cosmologie" and by the Ministry of Education through a DAGIC program.

REFERENCES

- Amram, P. 1991, Ph.D. thesis, Univ. Provence, Aix-Marseille
 Amram, P., Balkowski, C., Cayatte, V., Le Coarer, E., Marcelin, M., & Sullivan, W. T., III. 1991a, in *Distribution of Matter in the Universe*, ed. G. Mamon & D. Gerbal (Meudon: DAEC, Observatoire de Meudon), in press
 ———. 1991b, in *Clusters of Galaxies*, ed. A. Fabian (Cambridge: Cambridge Univ. Press), in press
 Amram, P., Le Coarer, E., Marcelin, M., Balkowski, C., Sullivan, W. T., III, & Cayatte, V. 1992, *A&AS*, 94, 175
 Bothun, G. D., Aaronson, M., Schommer, B., Mould, J., Huchra, J., & Sullivan, W. T., III. 1985, *ApJS*, 57, 423
 Bothun, G. D., Geller, M. J., Beers, T. C., & Huchra, J. P. 1983, *ApJ*, 268, 47
 Casertano, S., & van Gorkom, J. H. 1991, *AJ*, 101, 1231
 de Vaucouleurs, G., de Vaucouleurs, A., Corwin, H. G., Jr., Buta, R. J., Paturel, G., & Fouqué, P. 1991, *Third Reference Catalogue of Bright Galaxies* (New York: Springer)
 Distefano, A., Rampazzo, R., Chincarini, G., & de Souza, R. 1990, *A&AS*, 86, 7
 Dressler, A. J. 1980, *ApJ*, 236, 351
 Kennicutt, R. C., Jr., Bothun, G. D., & Schommer, R. A. 1984, *AJ*, 89, 1279
 Persic, M., & Salucci, P. 1991, *ApJ*, 368, 60
 Rubin, V. C., Whitmore, B. C., & Ford, W. K., Jr. 1988, *ApJ*, 333, 522 (RWF)
 Struble, M. F., & Rood, H. J. 1987, *ApJS*, 63, 543
 Sullivan, W. T., III. 1989, in *The World of Galaxies*, ed. H. G. Corwin, Jr., & L. Bottinelli (New York: Springer), 404
 Warner, P. J., Wright, M. C. H., & Baldwin, J. E. 1973, *MNRAS*, 163, 163
 Whitmore, B. C., Forbes, D. A., & Rubin, V. C. 1988, *ApJ*, 333, 542 (RWF)
 Zwicky, F., Herzog, E., Wild, P., Karpowicz, E., & Cowal, C. 1961–1968, *Catalogue of Galaxies and Clusters of Galaxies* (Pasadena: California Institute of Technology)